nature chemical biology

Green fluorescent proteins are light-induced electron donors

Alexey M Bogdanov[1], Alexander S Mishin[1], Ilia V Yampolsky[1], Vsevolod V Belousov[1], Dmitriy M Chudakov[1], Fedor V Subach[2], Vladislav V Verkhusha[2], Sergey Lukyanov[1] & Konstantin A Lukyanov[1]

Proteins of the green fluorescent protein (GFP) family are well known owing to their unique biochemistry and extensive use as *in vivo* markers. We discovered that GFPs of diverse origins can act as light-induced electron donors in photochemical reactions with various electron acceptors, including biologically relevant ones. Moreover, via green-to-red GFP photoconversion, this process can be observed in living cells without additional treatment.

GFP from the jellyfish *Aequorea victoria* and its artificial mutants are widely used in cell biology and biomedical research as genetically encoded fluorescent markers[1]. In the past decade, a number of GFP-like proteins have been found in diverse marine creatures—corals[2], copepods[3] and even lower chordates[4]. Detailed biochemical and crystallographic studies have shown a great diversity of chromophore structures that explain the wide spectral variations in GFP-like proteins[5–7].

In addition, diverse photoconversions have been demonstrated for fluorescent proteins[8,9]. In particular, in 1997, a noteworthy phenomenon was described: under anaerobic conditions, GFP and some of its mutants underwent efficient photoconversion into a red fluorescent state[10,11]. We use the term 'redding' to describe this photoconversion. Little is known about the structural basis of GFP redding. It occurs only if the oxygen concentration in the superfusing gas is below 1%[12]. Red fluorescence has excitation-emission maxima at 525 and 600 nm, respectively[10], and a fluorescence lifetime of 2.5 ns[13]. The red fluorescent form is stable for many hours in the absence of molecular oxygen, but it disappears quickly after re-oxygenation of the sample[10,12,13]. The structure and mechanisms of the formation of the GFP red state are unclear, and no hypothesis has been proposed.

Here, using confocal and fluorescence microscopy, we studied the influence of external agents on photobehavior of His-tagged EGFP immobilized on metal affinity beads (**Supplementary Methods** online). To our surprise, we observed very efficient green-to-red EGFP photoconversion when various electron acceptors were present in the medium. In contrast to anaerobic redding discussed above, EGFP redding with oxidants can be performed under both aerobic and anaerobic conditions. Such 'oxidative redding' was detected with $K_3[Fe(CN)_6]$ (potassium ferricyanide), benzoquinone (**1**) and 3-[4,5-dimethylthiazol-2-yl]-2,5-diphenyl tetrazolium bromide (MTT, **2**). In the presence of these chemicals, irradiation with a 488-nm laser line resulted in greatly accelerated bleaching of the green fluorescence and appearance of the red signal (**Fig. 1a**). As expected with MTT, a blue insoluble precipitate of the reduced formazan was detected on the irradiated areas of EGFP-containing beads. Notably, we observed substantially different degrees of dependence on oxidant concentration for rates of green fluorescence decrease and red fluorescence increase (**Fig. 1b**; **Supplementary Fig. 1** online). For all compounds tested, the EC_{50} (half maximal effective concentration) for EGFP bleaching was much (in some cases an order of magnitude) lower than that for the appearance of red fluorescence (**Supplementary Table 1** online). This difference suggests that EGFP redding can be a two-step process (**Fig. 1c**). Measurements of EGFP redding efficiency at different light intensities showed a linear dependence (**Supplementary Fig. 2** online). Thus, this photoconversion is a one-photon process, and we assume that a photon is absorbed at the first step of the proposed scheme. The nature of the red GFP state is unclear. A

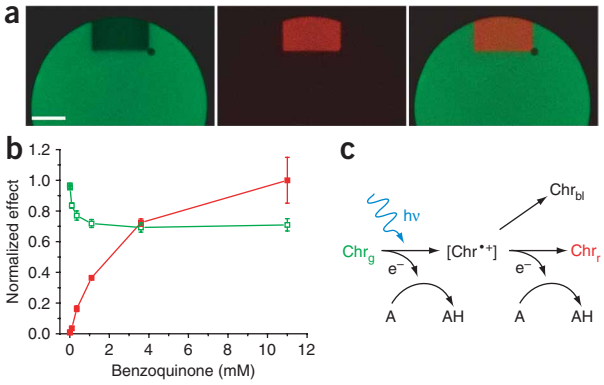

Figure 1 Oxidant-mediated green-to-red photoconversion of EGFP *in vitro*. (**a**) Confocal images of benzoquinone-mediated photoconversion of EGFP immobilized on a metal-affinity bead in green (left) and red (center) channels, and their overlay (right). A region on the upper side of the bead was preirradiated with a high-intensity 488-nm laser (1.5 W cm^{-2}). Scale bar, 20 μm. (**b**) Benzoquinone concentration dependences on green fluorescence decrease (green open squares) and red fluorescence increase (red closed squares) during oxidative redding of the immobilized EGFP. After one activating scan with 488-nm laser, remaining green fluorescence (normalized according to initial value) and originating red fluorescence (normalized according to maximal value) were measured and shown in the graph. Each data point is an average of three independent experiments. Error bars, s.d. (**c**) Proposed scheme of oxidative redding. In the first step, an excited green chromophore (Chr_g) donates one electron to an oxidant molecule (A). As a result, a short-lived intermediate ($Chr^{\bullet+}$) is formed. If it reacts with an electron acceptor during its lifetime, the final red fluorescent form (Chr_r) is formed; otherwise, the intermediate comes into a permanently bleached state (Chr_{bl}).

[1]Shemiakin-Ovchinnikov Institute of Bioorganic Chemistry, Moscow, Russia. [2]Department of Anatomy and Structural Biology, and Gruss-Lipper Biophotonics Center, Albert Einstein College of Medicine, Bronx, New York, USA. Correspondence should be addressed to K.A.L. (kluk@ibch.ru).

Received 1 December 2008; accepted 26 February 2009; published online 26 April 2009; doi:10.1038/nchembio.174

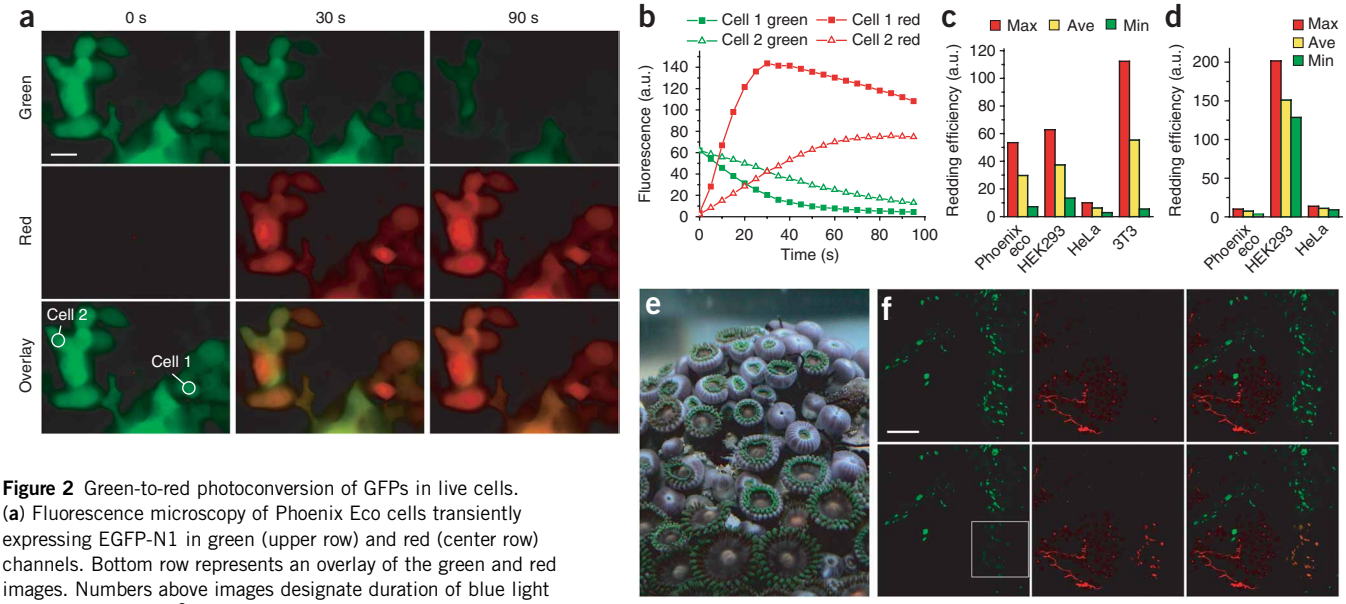

Figure 2 Green-to-red photoconversion of GFPs in live cells. (**a**) Fluorescence microscopy of Phoenix Eco cells transiently expressing EGFP-N1 in green (upper row) and red (center row) channels. Bottom row represents an overlay of the green and red images. Numbers above images designate duration of blue light irradiation (1 W cm^{-2}) that induces green-to-red photoconversion. Note the high heterogeneity of cells after 30 s of irradiation, which results in different colors on the overlaid image. Scale bar, 20 μm. (**b**) Quantification of fluorescence changes in two selected individual cells—cell 1 (filled squares) and cell 2 (open triangles)—marked in **a**. (**c**,**d**) Redding efficiency normalized according to initial green fluorescence level for designated cell lines transiently expressing EGFP in cytoplasm (**c**) or mitochondria (**d**). Maximal (red columns), average (yellow columns) and minimal (green columns) responses are shown for each cell line. (**e**,**f**) Green-to-red photoconversion in a live button polyp (*Zoanthus* sp.). (**e**) The *Zoanthus* specimen used in this work. (**f**) Confocal optical section through a tip of the native tentacle in green (left images) and red (center images) channels and their overlay (right images) before (upper row) and after (bottom row) photoconversion. Here green fluorescence is characteristic of the ectoderm cells, whereas endoderm cells contain the symbiotic algae *Zooxantella*, which resemble red spheres owing to chlorophyll fluorescence. Local photoconversion was induced in the region marked by a white square using irradiation with 100% 488-nm laser line (0.15 W cm^{-2}). Scale bar, 50 μm.

possible explanation is that, as a result of a two-electron oxidation, a DsRed-like red chromophore[14] is formed.

Oxidative redding of an EGFP solution in the presence of potassium ferricyanide in a cuvette showed red fluorescence spectra with excitation and emission maxima at 575 and 607 nm, respectively (**Supplementary Fig. 3a** online). The quantum yield of red fluorescence was about 0.05.

After oxidative redding at low concentrations of oxidants (for example, 1 μM benzoquinone), the red signal did not decrease for at least 1 h of observation. High concentrations (1 mM) of oxidants resulted in gradual decay of red fluorescence with a half-life of about 0.5 h. Fast disappearance of the red signal could be induced by addition of β-mercaptoethanol (**3**), while reduced glutathione (**4**) and ascorbate (**5**) did not affect stability of the red form. It is reasonable to expect reversibility of oxidative redding—that is, disappearance of red fluorescence would result in reappearance of green signal. However, experimentally we did not observe a proportional increase of green fluorescence during decay (either spontaneous or β-mercaptoethanol–induced) of the EGFP red form. Thus, the red chromophore converts into a spectrally undetectable form. It could be the GFP-like chromophore in a nonfluorescent state or a new unknown structure.

Next we tested biologically relevant electron acceptors. EGFP oxidative redding was found to occur in the presence of cytochrome *c* (ref. 15), flavin adenine dinucleotide (FAD, **6**), flavin mononucleotide (FMN, **7**), the FAD-containing flavoprotein glucose oxidase (which belongs to the same structural class as ubiquitous and abundant enzymes of cell redox homeostasis, such as glutathione reductase and thioredoxin reductase[16]) and nicotinamide adenine dinucleotide (NAD^+, **8**). So, excited EGFP was able to reduce compounds with an E_0 (the standard oxidation-reduction potential) of up to −0.32 V (**Supplementary Table 1**). Importantly, the appearance of reduced forms of cytochrome *c* and NAD^+ after EGFP oxidative redding was detected by absorption spectroscopy (**Supplementary Fig. 3b,c**). We estimated the yield of the redox reaction between EGFP and cytochrome *c* to be about 1.7, which suggests that EGFP oxidation is a two-electron process that can generate two reduced cytochrome *c* molecules per EGFP molecule. Notably, in the case of flavin-based oxidants, there was almost no difference in the EC_{50} calculated for the bleaching of green and activation of red fluorescence (**Supplementary Table 1**). It is likely that these oxidants are able to accept two electrons at once, thus promoting a one-step formation of the EGFP red state. Neither oxidized nor reduced glutathione, which are abundant components of the cell redox homeostasis system, induced green-to-red EGFP photoconversion (concentrations up to 30 mM have been tested).

Then we tested other GFPs of diverse origins, such as AcGFP1, TagGFP, zFP506, amFP486 and ppluGFP2, and found that all these proteins undergo oxidative redding (**Supplementary Table 2** online). However, the blue and cyan mutants of GFP (EBFP and ECFP) showed no oxidant-mediated photoconversion. Our recent study demonstrated that several diverse green and cyan fluorescent proteins can undergo anaerobic redding, but ECFP cannot[17]. Thus, for both oxidative and anaerobic redding, the chromophore should be based on tyrosine to be converted into the red state.

We next investigated whether EGFP can find appropriate electron acceptors and undergo green-to-red photoconversion within live mammalian cells. Indeed, green-to-red photoconversion was observed in a HEK293-derived Phoenix Eco cell line transiently transfected with an EGFP-N1 vector. Blue light irradiation resulted in a gradual

decrease of green fluorescence and a proportional increase of red fluorescence in living cells (**Fig. 2a**). Unexpectedly, individual cells demonstrated a very high variability of EGFP redding rate (**Fig. 2b**). No clear correlations between cell morphology or EGFP expression level and redding efficiency were revealed.

Then we compared the efficiency of EGFP redding in three cell lines: HEK293, HeLa and 3T3. We detected redding of different intensities, with very large differences between individual cells within each cell line (**Fig. 2c**).

Mitochondria represent the most reducing and redox-active compartment of mammalian cells[18]. Redding of EGFP targeted to mitochondria was tested in the Phoenix Eco, HEK293 and HeLa cell lines. EGFP-mito redding was efficient only in HEK293 cells, while other cell lines showed a much lower level of green-to-red photoconversion (**Fig. 2d**). Notably, the difference between individual cells was rather low. Generally, the rate of red fluorescence increase during the course of EGFP-mito redding was considerably faster than that of cytoplasmic EGFP redding under the same illumination conditions, even when compared to EGFP-N1–expressing cells with very high redding efficiency (**Supplementary Fig. 4** online). Thus, intracellular localization of EGFP strongly affects its redding, possibly due to known differences in redox potential and the composition and quantities of redox-active molecules in different cell compartments[18].

To test redding *in vivo*, we selected a button polyp (*Zoanthus* sp.) whose fluorescent proteins are well characterized[2,19–21]. A specimen with bright green tentacles (**Fig. 2e**) was analyzed by confocal microscopy. We found that cells with green fluorescence can be readily converted into a red state by brief irradiation with an intense 488-nm laser line (**Fig. 2f**). We believe that this photoconversion represents an oxidative redding of zFP506 in coral tissues. However, the presence of some still-unidentified photoconvertible fluorescent molecules that colocalize with zFP506 cannot be excluded.

Photoconversion described in the present work (oxidative redding) is clearly distinguishable from previously described green-to-red photoconversions of GFP variants under anaerobic conditions[10,11] (anaerobic redding). First, in contrast to anaerobic green-to-red photoconversion, during oxidative redding the red state is formed and is stable under normal aerobic conditions. Also, the red forms have different shapes and maxima of spectra, especially for excitation (525 and 575 nm for anaerobic and oxidative redding, respectively).

In the literature we found two classic models clearly resembling anaerobic GFP redding: a photoreduction of chlorophylls under anaerobic conditions[22,23], and an anaerobic photoconversion of flavoproteins[24] resulting in accumulation of stable semiquinoid radical forms that usually have red-shifted absorption spectra. Similarly, we propose that anaerobic GFP redding represents a photoreduction with formation of a stable radical state of GFP chromophore. This hypothesis explains the observed sensitivity of the photoconverted red GFP state to molecular oxygen. If so, GFPs can undergo both photoreduction (anaerobic redding) and photo-oxidation (oxidative redding) depending on external conditions—that is, the presence of oxygen and appropriate electron donors or acceptors.

Biological functions of fluorescent proteins remain incompletely understood[25]. The data presented here suggest a previously unknown GFP function: induction of a light-driven electron transfer. Such reactions may be involved in diverse cellular processes ranging from production of reductive equivalents (for example, $FADH_2$ or NADH) to general light sensing, if appropriate partners are connected with GFPs. Importantly, oxidative redding represents a common feature of many diverse GFPs. In fact, this is perhaps the most common type of photoconversion in GFP-like proteins. Thus, light-induced electron transfer may be considered a potential 'primary' function of the GFP ancestor, whereas other 'secondary' GFP functions, such as participation in bioluminescence and protection from sunlight, evolved later.

In addition, oxidative redding sheds light on the problem of multiple independent origins of red fluorescent proteins during evolution of the Anthozoa species, which is an example of convergent evolution at the molecular level[3,25]. From our data it is clear that various GFPs are 'accustomed' to light-induced oxidation into a red fluorescent state. Thus, it is reasonable to propose that some point mutations could further develop this ability toward light-independent maturation of the red chromophore.

In summary, the present work changes our general view of GFPs as passive light absorbers/emitters. Rather, an active role of GFPs in light-induced electron transfer should be kept in mind when one considers the biology of GFPs and potential applications. A number of new practical applications of GFP can be envisioned, such as redox monitoring in different cell compartments, redox monitoring of particular proteins, monitoring proximity to an electron acceptor, and light-induced manipulation of redox processes in living cells.

Note: Supplementary information and chemical compound information is available on the Nature Chemical Biology website.

ACKNOWLEDGMENTS

This work was supported by the MCB program of the Russian Academy of Sciences, the Russian Federal Agency for Science and Innovations (grant 02.513.12.3013), Howard Hughes Medical Institute (grant 55005618), the European Commission Sixth Framework Programme (LSHG-CT-2003-503259), the Russian Foundation for Basic Research (grants 07-04-12189-ofi and 09-04-00356-a), and the program "State Support of the Leading Scientific Schools" (NS-2395.2008.4). D.M.C. and K.A.L. are supported by the Russian Science Support Foundation and by grants from the president of the Russian Federation (MK-6119.2008.4 and MD-5815.2008.4). V.V.V. was supported by grant GM073913 from the US National Institutes of Health.

Published online at http://www.nature.com/naturechemicalbiology/
Reprints and permissions information is available online at http://npg.nature.com/reprintsandpermissions/

1. Lippincott-Schwartz, J. & Patterson, G.H. *Science* **300**, 87–91 (2003).
2. Matz, M.V. *et al. Nat. Biotechnol.* **17**, 969–973 (1999).
3. Shagin, D.A. *et al. Mol. Biol. Evol.* **21**, 841–850 (2004).
4. Deheyn, D.D. *et al. Biol. Bull.* **213**, 95–100 (2007).
5. Verkhusha, V.V. & Lukyanov, K.A. *Nat. Biotechnol.* **22**, 289–296 (2004).
6. Chudakov, D.M., Lukyanov, S. & Lukyanov, K.A. *Trends Biotechnol.* **23**, 605–613 (2005).
7. Pakhomov, A.A. & Martynov, V.I. *Chem. Biol.* **15**, 755–764 (2008).
8. Lukyanov, K.A., Chudakov, D.M., Lukyanov, S. & Verkhusha, V.V. *Nat. Rev. Mol. Cell Biol.* **6**, 885–891 (2005).
9. Shaner, N.C., Patterson, G.H. & Davidson, M.W. *J. Cell Sci.* **120**, 4247–4260 (2007).
10. Elowitz, M.B., Surette, M.G., Wolf, P.E., Stock, J. & Leibler, S. *Curr. Biol.* **7**, 809–812 (1997).
11. Sawin, K.E. & Nurse, P. *Curr. Biol.* **7**, R606–R607 (1997).
12. Takahashi, E. *et al. Am. J. Physiol. Cell Physiol.* **291**, C781–C787 (2006).
13. Jakobs, S., Schauss, A.C. & Hell, S.W. *FEBS Lett.* **554**, 194–200 (2003).
14. Gross, L.A., Baird, G.S., Hoffman, R.C., Baldridge, K.K. & Tsien, R.Y. *Proc. Natl. Acad. Sci. USA* **97**, 11990–11995 (2000).
15. Moore, G.T. & Pettigrew, G.W. *Cytochrome c: Evolutionary, Structural and Physicochemical Aspects* (Springer-Verlag, New York, 1990).
16. Dym, O. & Eisenberg, D. *Protein Sci.* **10**, 1712–1728 (2001).
17. Kiseleva, Iu.V., Mishin, A.S., Bogdanov, A.M., Labas, Iu.A. & Luk'ianov, K.A. *Bioorg. Khim.* **34**, 711–715 (2008).
18. Go, Y.M. & Jones, D.P. *Biochim. Biophys. Acta* **1780**, 1273–1290 (2008).
19. Labas, Y.A. *et al. Proc. Natl. Acad. Sci. USA* **99**, 4256–4261 (2002).
20. Remington, S.J. *et al. Biochemistry* **44**, 202–212 (2005).
21. Pletneva, N. *et al. Acta Crystallogr. D Biol. Crystallogr.* **62**, 527–532 (2006).
22. Krasnovsky, A.A. *Dokl. Akad. Nauk SSSR* **60**, 421–424 (1948).
23. Krasnovsky, A.A. *Annu. Rev. Plant Physiol.* **11**, 363–410 (1960).
24. Massey, V. & Palmer, G.H. *Biochemistry* **5**, 3181–3189 (1966).
25. Alieva, N.O. *et al. PLoS One* **3**, e2680 (2008).